

# Alcohol degradation of anhydride-cured epoxy resin insulating materials containing SiO<sub>2</sub> filler

Cite as: AIP Advances 15, 065007 (2025); doi: 10.1063/5.0273088

Submitted: 28 March 2025 • Accepted: 8 May 2025 •

Published Online: 4 June 2025



View Online



Export Citation



CrossMark

Xu Zhang,<sup>1</sup> Chengjie Li,<sup>1</sup> Xianming Ye,<sup>2</sup> Xiaoxing Zhang,<sup>1</sup> Eric Maluta,<sup>3</sup> and Yunjian Wu<sup>1,a)</sup>

## AFFILIATIONS

<sup>1</sup>Hubei Engineering Research Center for Safety Monitoring of New Energy and Power Grid Equipment, Hubei University of Technology, Wuhan, Hubei 430068, People's Republic of China

<sup>2</sup>Department of Electrical, Electronic, and Computer Engineering, University of Pretoria, Gauteng, Pretoria 0028, South Africa

<sup>3</sup>Green Technology Confucius Institute, University of Venda, Thohoyandou, Limpopo 0950, South Africa

<sup>a)</sup>Author to whom correspondence should be addressed: [wuyunjian@hbut.edu](mailto:wuyunjian@hbut.edu)

## ABSTRACT

The anhydride-cured epoxy resin with silica micro-powder (SAE) is widely used in electrical equipment due to its excellent properties. However, its three-dimensional network structure makes degradation and recycling difficult. Conventional disposal methods, such as incineration or landfill waste resources, harm the environment. Therefore, it is crucial to develop a mild degradation and recycling method for epoxy resin. In this study, after evaluating the electrical, mechanical, and thermal properties of SAE, we achieved efficient and mild alcoholysis of high filler content (50%) SAE. This was done using K<sub>3</sub>PO<sub>4</sub> as a catalyst and ethanol as a solvent, with the reaction conducted at 120 °C for 3 h. We also explored degradation optimization at different temperatures, with varying water and filler contents. Results showed a degradation efficiency of nearly 100% under these conditions. Raising the temperature moderately and adding a small amount of water were found to boost the degradation efficiency. The insolubility of K<sub>3</sub>PO<sub>4</sub> in ethanol enabled effective separation and reuse of the catalyst and filler. FTIR analysis confirmed the chemical structure of the degradation products, showing their recyclability. This degradation method allows for efficient degradation of SAE while maintaining or even enhancing its properties compared to pure epoxy resin.

© 2025 Author(s). All article content, except where otherwise noted, is licensed under a Creative Commons Attribution-NonCommercial-NoDerivs 4.0 International (CC BY-NC-ND) license (<https://creativecommons.org/licenses/by-nc-nd/4.0/>). <https://doi.org/10.1063/5.0273088>

## I. INTRODUCTION

Epoxy resin, known for its excellent mechanical properties, electrical insulation, and chemical stability, is widely used in electrical equipment.<sup>1</sup> However, its three-dimensional network structure after curing makes it difficult to recycle.<sup>2,3</sup> Generally, discarded epoxy resin materials are still disposed of by incineration or landfill; this not only wastes valuable resources but also causes serious environmental pollution.<sup>4</sup> Moreover, the degradation conditions for epoxy resin are harsh and complex, and the resulting degradation products have a broad molecular weight distribution, which reduces the value of the recycled materials,<sup>5</sup> further increasing the difficulty of the recycling process.

In recent years, with the increasing strictness of environmental regulations and the advancement of sustainable development concepts, researchers have gradually focused on the degradation of epoxy resin under mild conditions.<sup>6</sup> Although methods such

as physical recycling or energy recovery have been developed to improve the recycling rate, the efficiency of recycling remains low. Chemical recycling is considered a more promising approach because it can produce useful chemicals and has the potential for a circular economy;<sup>7</sup> traditional chemical degradation methods, such as hydrolysis, alcoholysis, and amination, have achieved the degradation of epoxy resins to a certain extent; however, there are problems, such as harsh reaction conditions and difficult separation of degradation products. For this reason, researchers have attempted to achieve a more efficient and environmentally friendly degradation pathway through catalyst optimization, solvent system modification, and stepwise degradation strategies. Zhang *et al.* used an organocatalyst, N-methyl-4-piperidinol to degrade methylcyclohexene 1,2-dicarboxylic anhydride-cured (MeTHPA) epoxy resins in ethylene glycol, which resulted in the separation of the catalyst products and effective recovery of the ethylene glycol and the catalyst;<sup>8</sup> however, the degradation conditions are demanding (1 h reaction at

180 °C).<sup>9</sup> Zhao *et al.* degraded an epoxy resin by microwave-assisted catalytic degradation of diethylenetriamine (DETA) at 130 °C for 50 min. DETA acted as a catalyst, reactant, and solvent, and the product of the ammonization was reused as a curing agent in the new epoxy system directly together with the excess of DETA; however, the new resin could not be recycled by using the same DETA degradation system.<sup>10</sup>

Alcoholysis, as a commonly used degradation method, involves breaking the cross-linked ester bonds in epoxy resin through ester exchange reactions catalyzed by a catalyst, thereby achieving decomposition at relatively low temperatures. However, in the mainstream degradation methods currently available, there is limited research on the degradation of epoxy resin containing SiO<sub>2</sub> used in electrical equipment. Most studies to date have primarily focused on recovering materials, such as carbon fibers or copper foils, from epoxy composites.<sup>11–13</sup>

Given the current situation, this study focuses on the degradation behavior of SAE and explores its degradation pathways under mild conditions. We conducted necessary performance characterizations of SAE with different SiO<sub>2</sub> contents. Using K<sub>3</sub>PO<sub>4</sub> as a catalyst and ethanol as a solvent, we successfully achieved efficient degradation of epoxy resin composites with high SiO<sub>2</sub> content after reacting at 120 °C for 3 h. We also systematically analyzed the chemical structure and properties of the degradation products and realized the recovery of the catalyst and filler, providing a valuable reference for the recycling and utilization of SAE.

## II. PREPARATION OF SAE

### A. Materials of SAE

Figure 1 demonstrates the preparation process and the alcoholysis process of the materials, where Fig. 1(a) shows all the processes of preparation and alcoholysis and Fig. 1(b) shows the material changes before and after the alcoholysis reaction process.

DGEBA, as the epoxy monomer, was purchased from Bluesstar New Material Co. MeTHPA, as the curing agent, was purchased from Aladdin Company; DMP-30, as the accelerator of the curing process, was purchased from Aladdin Company; and KH-560, as

the coupling agent, was purchased from Nanjing Glass Fiber Company. SiO<sub>2</sub> was purchased from Ming-Ri Nanomaterials Ltd. as a filler for the epoxy resin. Anhydrous ethanol with 99.5% purity was used as a solvent in the degradation process and was purchased from Chengdu Cologne Chemical Co. K<sub>3</sub>PO<sub>4</sub> acted as a catalyst in the degradation process and was purchased from Adams Company. All these reagents were used directly since purchase without further purification.

### B. Preparation of SAE

DGEBA, MeTHPA, and DMP-30 were mixed into a mixture with a mass ratio of 10:7.04:0.104.<sup>10</sup> SiO<sub>2</sub> was pretreated using KH-560 prior to the curing process, and the pretreated SiO<sub>2</sub> was added to the mixture in weight ratios of 10, 20, 30, 40, 45, and 50 wt. %. They were stirred mechanically and, after mixing well, vacuumed for 30 min, the PTFE molds were sprayed with an appropriate release agent beforehand, and then, the mixture with the addition of SiO<sub>2</sub> was poured into the PTFE molds that had been preheated for 5–10 min. The molds were placed in an oven, and the samples were obtained after being heated at 120 °C for 2 h, and then at 150 °C for 4 h. When the samples were cooled to room temperature, the obtained samples were demolded.

## III. EXPERIMENTAL METHODS

### A. Chemical structure

Fourier transform infrared (FTIR) spectra were recorded using a NICOLET 6700 FTIR spectrometer manufactured by Thermoelectron Corporation, USA. The KBr powder and SAE powders with different SiO<sub>2</sub> contents were ground into a mixture of the appropriate size in a mass ratio of 40:1 and pressed for 15 min to prepare a thin slice sample, which would be in the range of 450–4000 cm<sup>-1</sup>, where the infrared absorption peaks of SAE samples were recorded.

### B. Electrical properties

Volume resistivity was measured by a 6517B Electrostatic Meter/High Resistance Meter combined with a three-electrode

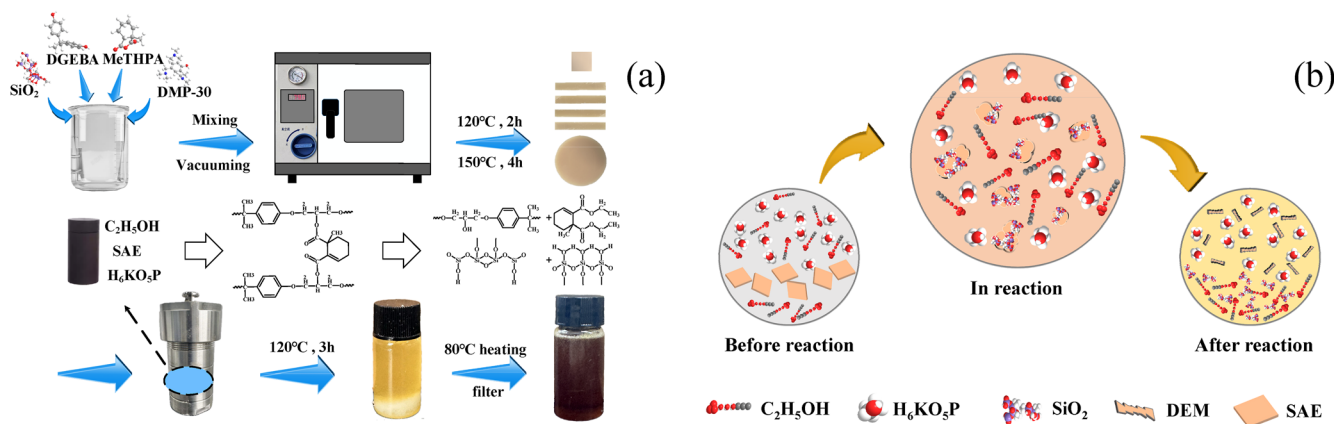


FIG. 1. (a) Preparation and alcoholysis. (b) Substance changes before, during, and after the alcoholysis reaction process.

fixture from Keithley, USA. To ensure accuracy and reliability, at least 30 measurements were made on SAE samples with different SiO<sub>2</sub> contents.

The AC breakdown strength was measured by an AC breakdown test rig. The AC breakdown test was performed using a pair of ball electrodes with a diameter of 20 mm and a voltage slope of 500 V/s. At least ten tests were performed on SAE samples with different SiO<sub>2</sub> contents. During the tests, the samples and electrodes were completely immersed in an insulating oil medium. All the samples were of disk type with a diameter of 40 mm and all with a thickness of 1 mm, and all the measurements of the samples were carried out in a room temperature environment.

### C. Mechanical properties and thermal properties

Tensile mechanical strength produced by American Instruments 3343 was measured by an electromechanical testing system. The SAE samples with different SiO<sub>2</sub> contents were all sized to be  $5 \times 1.3 \times 0.3 \text{ cm}^3$ ,<sup>14</sup> and the tensile loading rate was 5 mm/min.

The DSC curves were measured by a differential scanning calorimeter. The samples were first held at 150 °C for 5 min to eliminate thermal history, then 10 mg of SAE samples with different SiO<sub>2</sub> contents were rapidly cooled to ~100 °C at a rate of 50 °C/min for 5 min, then heated from 50 to 250 °C at a rate of 20 °C/min, and finally cooled to room temperature. The purge gas used during the analysis was nitrogen at a flow rate of 50 ml/min.

The TGA curves were measured by a GA Q500 thermal analyzer manufactured by TA Instruments, USA. The analyzer was measured in constant heating rate mode, heating at a rate of 30 °C/min. The operating temperature range was from room temperature to 800 °C and was carried out in a nitrogen atmosphere with a nitrogen purge rate of 60 ml/min. The weight of all measured samples was about 10 mg.

## IV. EXPERIMENT RESULTS

### A. FTIR results

FTIR was used to verify the composition of the products and to investigate the effect of SiO<sub>2</sub> on the functional groups of the epoxy resin. Due to the presence of impurity peaks, the analysis emphasized only the characteristic peaks that best reflect the structure of SAE samples with different SiO<sub>2</sub> contents, and the results are shown in Fig. 2. In the SAE samples with different SiO<sub>2</sub> contents, the characteristic peak of hydroxyl group (–OH) is in the region of 3200–3600 cm<sup>–1</sup>, which is related to the –OH stretching vibration.<sup>15</sup> The characteristic peak for carbon–hydrogen (C–H) is in the region of 2800–3000 cm<sup>–1</sup> and is usually associated with the saturated C–H stretching vibration.<sup>16</sup> The characteristic peak for esters is in the region of 1700–1800 cm<sup>–1</sup> and is associated with the –COO– stretching vibration. The characteristic peak of the ether is in the region of 1000–1300 cm<sup>–1</sup> and is related to the stretching vibration of –C–O–C–.<sup>17</sup> As can be seen from the figure, the intensity of the absorption peaks of the different functional groups changes as the weight percentage increases, with the absorption peaks of –OH and C–H likely to be more pronounced in higher weight percentages of the samples, and the absorption peaks of the ester and the ether being in the lower wavelength region, and the intensity of these peaks is

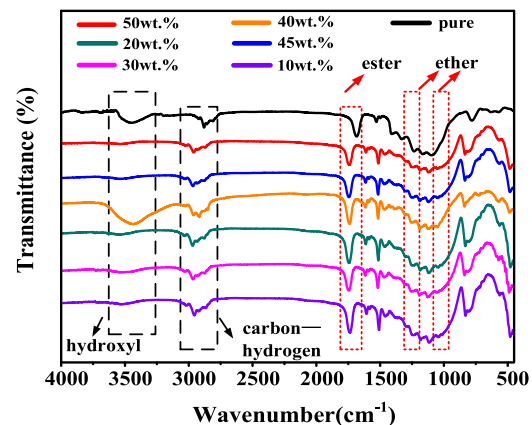


FIG. 2. FTIR spectra of SAE with different SiO<sub>2</sub> contents.

likely to increase as these functional groups are increased in the samples. In addition to this, the absorption peaks at 1609 and 1582 cm<sup>–1</sup> at 50 wt. % are related to the C=C and C–C stretching vibrations,<sup>18</sup> respectively, the weak intensity band at 1650 cm<sup>–1</sup> is related to the N–H functional group, and the weak absorption peak at 3400 cm<sup>–1</sup> is related to Si–OH.<sup>19,20</sup>

All these FTIR observations showed that no new bonds appeared between the filler and the epoxy resin,<sup>15</sup> and the pure epoxy resin samples without SiO<sub>2</sub> have a similar chemical structure to the SAE samples, thus verifying the feasibility of the SAE samples with a certain amount of SiO<sub>2</sub> content for the alcoholysis method.<sup>12,21–23</sup>

### B. Electrical parameters

Figure 3(a) demonstrates the effect of different SiO<sub>2</sub> contents on the resistivity of SAE samples. With the increase in SiO<sub>2</sub> content, the resistivity shows an overall decreasing trend, which indicates that increasing the content of SiO<sub>2</sub> can reduce the resistivity of the material and SiO<sub>2</sub> in the material changes the conductive properties of the material; This trend may be related to a kind of ionic transport modeling of the distribution of SiO<sub>2</sub> in the material, the size of the particles, and the surface properties of the material,<sup>23,24</sup> which decreased from about  $2.0 \times 10^{16} \Omega \text{ cm}$  at 0 wt. % to about  $1.0 \times 10^{16} \Omega \text{ cm}$  at 50 wt. %. The median resistivity was about  $3.0 \times 10^{16} \Omega \text{ cm}$  with the addition of 20 wt. % SiO<sub>2</sub> and about  $1.0 \times 10^{16} \Omega \text{ cm}$  with the addition of 50 wt. % SiO<sub>2</sub>. However, most of the SAE's resistivities do not decrease much relative to the pure epoxy resin, and most of the resistivity values are still higher than the lowest resistivity value of  $10^{15} \Omega \text{ cm}$  reported in reference to the relevant standards.<sup>25</sup>

Figure 3(b) demonstrates the effect of different SiO<sub>2</sub> contents on the relative permittivity of SAE samples. The relative dielectric constants of the samples all decreased with the increase in frequency, which is due to the difficulty of dipole orientation polarization following the electric field at high frequency, resulting in the decrease of polarization strength and relative dielectric constant.<sup>26,27</sup> On the other hand, most of the relative dielectric constants of SAE are higher than those of pure epoxy materials, which is probably because

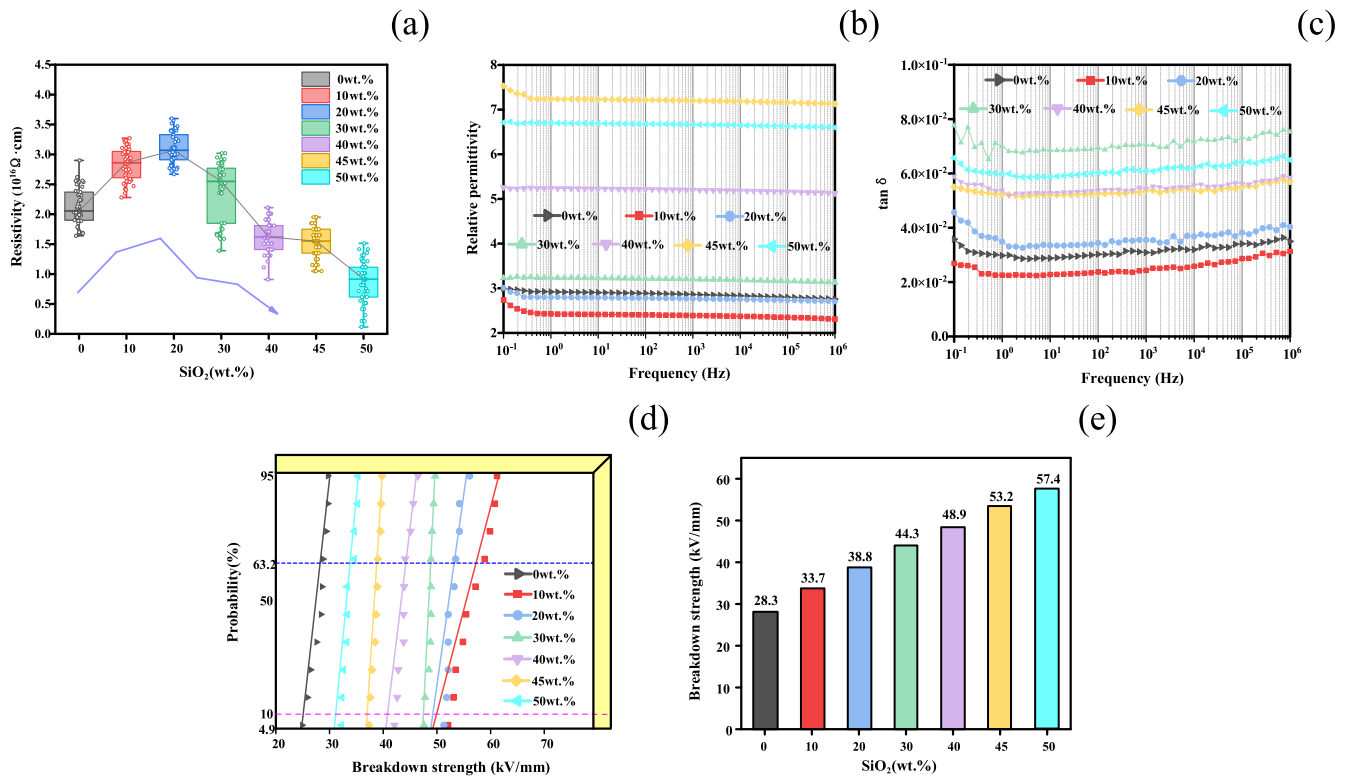


**FIG. 3.** (a) Effect of SiO<sub>2</sub> content on SAE resistivity. (b) Effect of SiO<sub>2</sub> content on SAE relative permittivity. (c) Effect of SiO<sub>2</sub> content on SAE tan  $\delta$  values. (d) Effect of SiO<sub>2</sub> content on SAE breakdown probability. (e) Effect of SiO<sub>2</sub> content on SAE breakdown strength.

SiO<sub>2</sub> increases the number of polar molecules and polarity in the system.<sup>27</sup>

In the low-frequency region of 10<sup>-1</sup> to 10<sup>2</sup> Hz, the relative permittivity of the samples with different SiO<sub>2</sub> contents varies greatly. In addition, 45 and 50 wt.% samples have higher relative permittivity, while 10 wt.% samples have the lowest, and in the high-frequency region of 10<sup>3</sup>–10<sup>6</sup> Hz, the difference in relative permittivity of the samples with different SiO<sub>2</sub> contents decreases, and the relative permittivity of all samples tends to be constant. The relative permittivity of pure epoxy resin is relatively low and does not change much in the whole frequency range, indicating that its dielectric properties are relatively stable. In the low-frequency region, all types of polarization mechanisms, including electronic polarization, ionic polarization, interfacial polarization, and dipole polarization work, result in a high relative permittivity, and in the high-frequency region, due to the rapidly varying electric field, only the electronic polarization is capable of responding quickly, while the other polarization mechanisms gradually drop out of the response, resulting in the decrease of the relative permittivity.<sup>27</sup> For engineering applications, the relative dielectric constants of all SAE samples range from 2.5 to 7.5 in the 10<sup>-1</sup>–10<sup>6</sup> Hz band, which are as good as those of pure epoxy resins for engineering applications.<sup>28</sup>

Figure 3(c) demonstrates the effect of different SiO<sub>2</sub> content on the SAE samples on the loss factor tan  $\delta$ . The loss factor tan  $\delta$  reflects

the heat generated by the material during polarization and is one of the important parameters to measure the performance of insulating materials. In the low-frequency region of 10<sup>-1</sup>–10<sup>2</sup> Hz, all the samples have higher values of tan  $\delta$ , indicating that the polarization loss of the material is higher at low frequencies. As the frequency increases, the tan  $\delta$  values gradually decrease, which indicates that the polarization loss of the material decreases at high frequencies. In the low-frequency region, the samples with 30 and 50 wt.% have the highest tan  $\delta$  values, which indicates that the polarization loss of these samples is larger at low frequencies, and the tan  $\delta$  values of the samples with different SiO<sub>2</sub> contents are gradually close to each other with the increase in frequency, which indicates that the effect of the different SiO<sub>2</sub> contents on the polarization loss of the material decreases at high frequencies. This indicates that the effect of different SiO<sub>2</sub> content on the polarization loss of the material decreases at high frequencies. In the high-frequency region of 10<sup>4</sup>–10<sup>6</sup> Hz, the tan  $\delta$  values of all the samples tend to be stable with little difference. The relatively low tan  $\delta$  values of pure epoxy resin in the whole frequency range, with little variation, indicate that it has a good insulating property because it generates less heat during the polarization process. In the low-frequency region, electronic polarization and ionic polarization may dominate, resulting in higher tan  $\delta$  values. As the frequency increases, other types of polarization, such as interfacial polarization and dipole polarization, may be excited; however, due to the increase in frequency, the response of these polarization

mechanisms may not be able to keep up with the change in the electric field, resulting in lower  $\tan \delta$  values.<sup>29</sup> In consideration of engineering applications, in the low-frequency region, the 30 and 50 wt. % samples have low and close  $\tan \delta$  values due to higher  $\tan \delta$  values, and in the high-frequency region, all the samples have low and close  $\tan \delta$  values, which indicates that they have better insulation properties at high frequencies and are all suitable for high-frequency voltage operating conditions.<sup>30</sup>

Figures 3(d) and 3(e) demonstrate the effect of different SiO<sub>2</sub> contents on the breakdown strength of SAE samples against industrial frequency AC, respectively. Each SiO<sub>2</sub> content in the figure corresponds to a curve showing the Weibull probability distribution at a specific breakdown strength. With the increase in SiO<sub>2</sub> content, the distribution of breakdown strength changes, indicating that the addition of SiO<sub>2</sub> has a significant effect on the insulating properties of the material.

As shown in the sample breakdown plots in Fig. 4, the cracks at the breakdown location exhibited a change from point-like cracks when the SiO<sub>2</sub> content in the SAE was changed to a higher level, a phenomenon that may be related to the weakening of the brittleness of the SAE samples. The breakdown data were in the range of 25–60 kV/mm, and the breakdown strength corresponding to the 63.2% probability increased with the increase in SiO<sub>2</sub> content, indicating the improvement of the insulating properties of the material. The breakdown strength corresponding to 63.2% probability for pure epoxy resin is about 25 kV/mm, and when

the SiO<sub>2</sub> content is increased to 50 wt. %, the breakdown strength corresponding to 63.2% probability increases to about 57.4 kV/mm, showing a significant improvement. As can be seen from the inset, the highest value is reached at 50 wt. % SiO<sub>2</sub> at 63.2% probability with increasing SiO<sub>2</sub> content. The instantaneous breakdown is mainly related to the concentration of free carriers and the mobility of free carriers in the electric field, and when tiny particles are doped into the polymer matrix, interaction zones are formed around them, which introduce deep-trapped sites at the matrix–particle interface, a phenomenon that can be explained by a structural modeling.<sup>31</sup> The addition of SiO<sub>2</sub> may affect the polarization mechanism and insulating properties of the material by introducing more polar molecules and trap energy levels that may trap free charge carriers and reduce their mobility, thus increasing the breakdown strength of the material.<sup>32</sup> The results of this study show that the SAE samples retain excellent insulating properties relative to pure epoxy resin and comply with the relevant standards.<sup>28</sup>

### C. Mechanical strengths and thermal

Figure 5(a) demonstrates the effect of different SiO<sub>2</sub> contents on the tensile strength of SAE samples. With the increase in SiO<sub>2</sub> content, both the maximum and minimum tensile strengths showed certain trends. During the increase in SiO<sub>2</sub> content from 0 to 45 wt. %, the maximum tensile strength first increased and then slightly decreased, while the minimum tensile strength showed a gradual

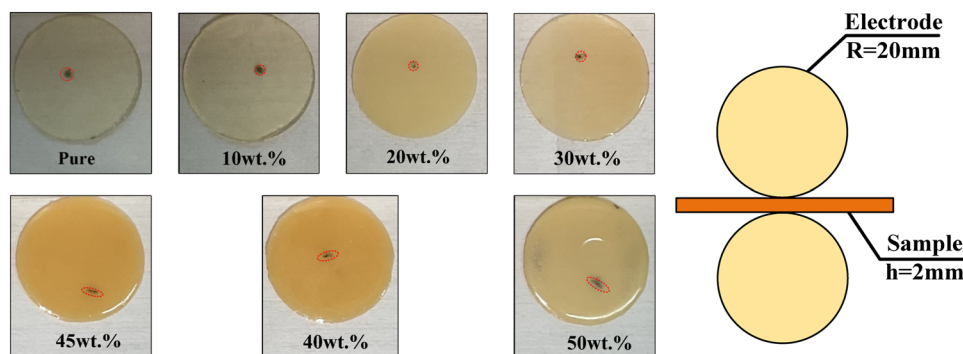


FIG. 4. AC breakdown diagram and sample experiments.

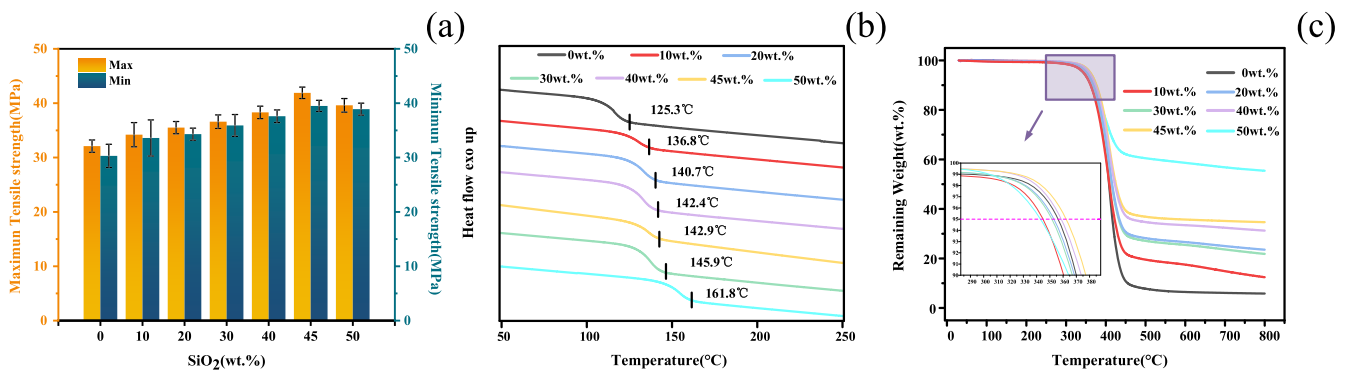


FIG. 5. (a) Effect of SiO<sub>2</sub> content on SAE tensile strengths. (b) Effect of SiO<sub>2</sub> content on DSC curves. (c) Effect of SiO<sub>2</sub> content on TGA curves.

increasing trend. As shown in the figure, a moderate amount of SiO<sub>2</sub> filling can improve the tensile strength of epoxy composites; however, too much SiO<sub>2</sub> filling may lead to a decrease in the tensile strength. This may be because a moderate amount of SiO<sub>2</sub> filling can increase the rigidity and strength of the material; however, too much SiO<sub>2</sub> filling may lead to an increase in stress concentration and defects inside the material, which will reduce the tensile strength. The maximum tensile strength of the pure epoxy resin is 30 MPa. When the SiO<sub>2</sub> content is increased to 45 wt. %, the maximum tensile strength reaches the highest value of 42 MPa. At 50 wt. % SiO<sub>2</sub>, the maximum tensile strength slightly decreases to 40 MPa. The minimum tensile strength of the pure epoxy resin is about 30 MPa. With the increase in the SiO<sub>2</sub> content, the minimum tensile strength increases gradually, and the maximum tensile strength of the pure epoxy resin is about 30 MPa. The minimum tensile strength of pure epoxy resin is about 30 MPa. With the increase in SiO<sub>2</sub> content, the minimum tensile strength increases gradually and reaches the maximum value of about 39 MPa at 45 wt. % SiO<sub>2</sub>, and the minimum tensile strength slightly decreases to 38 MPa at 50 wt. % SiO<sub>2</sub> but still meets the standard.<sup>30</sup>

Figure 5(b) demonstrates the effect of different SiO<sub>2</sub> content on the T<sub>g</sub> of SAE samples. Compared to the pure epoxy resin sample, the T<sub>g</sub> of the SAE sample with 45 wt. % SiO<sub>2</sub> content increased by 36.5 °C, as shown by the classification of the insulation according to the relevant standards;<sup>33</sup> for samples with up to 50% SiO<sub>2</sub> content, they can be used as normal engineering thermal insulating epoxy resins due to their T<sub>g</sub> values higher than 90 °C.

Figure 5(c) demonstrates the effect of different SiO<sub>2</sub> contents on the thermal stability of SAE samples. Compared with pure epoxy resin, the thermal stability of SAE with low SiO<sub>2</sub> content decreased and its 5% heat loss decomposition temperature was lower than that of pure epoxy resin, and the thermal stability of SAE with high SiO<sub>2</sub> content increased and its 5% heat loss decomposition temperature was higher than that of pure epoxy resin. However, all the maximum heat loss peaks remain around 400 °C, showing good thermal stability and meeting the needs of most engineering epoxy resins.

## V. BACKGROUND TO THE STUDY AND THE NEED FOR DEGRADATION

In Sec. IV C, we systematically evaluated the electrical, mechanical, and thermal properties of epoxy composites containing SiO<sub>2</sub> fillers. The results show that the composites exhibit comparable or even superior properties to those of pure epoxy resins even under conditions of high SiO<sub>2</sub> content (50%) filling. This finding suggests that epoxy resin composites with SiO<sub>2</sub> fillers have great potential for application in the field of high-performance electrical equipment materials. However, despite its excellent performance, the study of SiO<sub>2</sub> containing epoxy resins in electrical equipment mainly focuses on its performance, and the degradation study of this kind of SiO<sub>2</sub> containing filler epoxy resins is still relatively scarce, especially the degradation paths under mild conditions; the related studies are still in the preliminary stage of exploration.<sup>35–37</sup> This status quo contrasts with the widespread use of epoxy resins containing SiO<sub>2</sub> fillers.

Therefore, the development of a mild and efficient degradation method that not only realizes the complete degradation of SiO<sub>2</sub>-filled epoxy resins but also recovers valuable fillers and degradation

products is of great significance in promoting the sustainable treatment of epoxy resin wastes. In this study, we aimed to fill this research gap by using K<sub>3</sub>PO<sub>4</sub> as a catalyst and ethanol as a solvent to realize the efficient degradation of high-content SiO<sub>2</sub>-filled epoxy resin under mild conditions. This method not only provides a new idea for the degradation of SiO<sub>2</sub>-containing filler epoxy resins but also provides an experimental basis for the efficient recovery and reuse of resources. In the subsequent Sec. V, we will explore the mechanism of this degradation system in detail and further optimize the reaction conditions to achieve a more efficient and environmentally friendly degradation pathway.

## VI. ALCOHOLYSIS OF SAE

The mechanism of alcoholysis of SAE is shown in Fig. 6. The pretreated SiO<sub>2</sub>, as shown in Fig. 6(a), is mainly dispersed in the epoxy resin matrix as a filler of physical reinforcement material, which is inert in nature, and the filler does not directly participate in the alcoholysis reaction of the epoxy resin.<sup>34</sup> Figure 6(b) shows the encapsulation and dispersion relationship between the epoxy resin and the pretreated SiO<sub>2</sub>. Alcoholysis usually involves an ester exchange reaction, which effectively breaks the ester bond, resulting in the degradation of the epoxy resin into smaller oligomers. Figure 6(c) shows the reactive substances involved in this ester exchange reaction, which is the curing reaction between the epoxy resin monomer and the anhydride curing agent to form the epoxy product with a cross-linking structure. Figure 6(d) shows the reaction of K<sub>3</sub>PO<sub>4</sub> with the alcohol (ROH) to form the negative alcohol ion (RO<sup>-</sup>); RO<sup>-</sup> is the main reactive substance to attack the ester bond.<sup>38</sup> In this chemical transformation, as shown in Fig. 6(e), RO<sup>-</sup> preferentially attacks the ester bond, which breaks under the action of RO<sup>-</sup> to produce the corresponding alcoholysis product. Through this reaction, new esters are formed, and hydroxyl groups are released; the molecular structure formula of which is shown in Fig. 6(f). The final degradation product is a key step in the recycling and reuse of epoxy resins, which can partially replace the DGEBA base material for the production of new epoxy resins, contributing to a more sustainable use of the material and enhancing a multi-recycling and sustainable material life cycle.<sup>11,25,38</sup>

Rectangular block SAE samples of 20 × 20 × 5 mm<sup>3</sup> were obtained and used for alcoholysis reaction. SAE, anhydrous ethanol, and K<sub>3</sub>PO<sub>4</sub> were mixed in a reactor in a mass ratio of 3:30:1 and heated at 120 °C for 3 h to obtain the degradation solution.<sup>11</sup> The solution was placed in a vacuum pump evaporator and vacuumed, and 45 °C was maintained to evaporate the ethanol and obtain a mixture of degradation product and SiO<sub>2</sub>, which was separated from the degradation product and SiO<sub>2</sub> by passing through a filter and then dried for an appropriate period of time to obtain SiO<sub>2</sub> powder. As shown in Fig. 7, the characteristic peaks corresponding to the ether bonds in the product skeleton before and after degradation were present in the spectral analyses at 1249 and 1010 cm<sup>-1</sup>, which indicated that the structure of the skeleton before and after the reaction of the epoxy resin remained unchanged. The decrease in the intensity of the carbonyl peak at 1790 cm<sup>-1</sup> after degradation indicates the destruction of cross-linking sites within SAE, which proves that SAE has been successfully alcoholized by the degradation system of anhydrous ethanol and K<sub>3</sub>PO<sub>4</sub>.

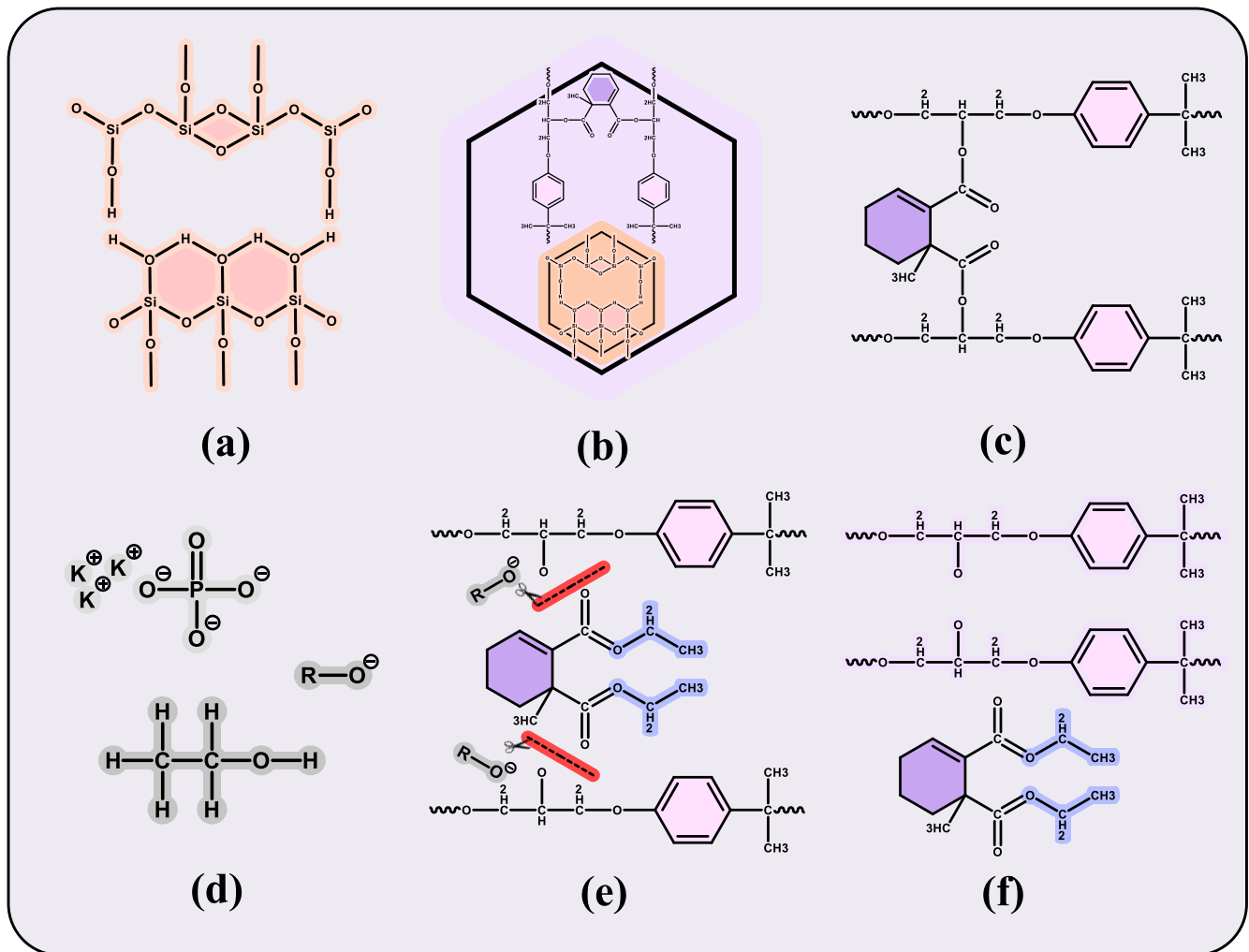


**FIG. 6.** (a) Dispersion of pretreated SiO<sub>2</sub> in the epoxy matrix. (b) Encapsulation and dispersion relationship between epoxy resin and pretreated SiO<sub>2</sub>. (c) Reactive substances in ester exchange reactions. (d) K<sub>3</sub>PO<sub>4</sub> reacts with alcohols to form negative alcohol ions RO<sup>-</sup>. (e) RO<sup>-</sup> attack ester key. (f) New ester and release of hydroxyl groups.

However, during the actual degradation process, Fig. 8(a) demonstrates the effect of water content on the degradation degree. An appropriate increase in the water content in ethanol or K<sub>3</sub>PO<sub>4</sub> improved the catalytic degradation efficiency, and after the ethanol solvent adsorbed a small amount of water in the air, the solubility of K<sub>3</sub>PO<sub>4</sub> was increased, which allowed it to participate in the degradation reaction more efficiently, thus accelerating the degradation process. However, when the water content was further increased, the degree of degradation decreased instead because the degradation products were poorly soluble in water, and too much water would reduce the solvent properties of the system. SAE itself was not wetting, and too much water would impede the degradation reaction. Figure 8(b) demonstrates the effect of temperature on the degree of degradation. An appropriate increase in temperature

during degradation improves the degradation efficiency. The solubilization of SAE by ethanol was enhanced at higher temperatures, which improved the ability of the catalyst and ethanol molecules to penetrate into the interior of SAE, thus increasing the contact area of the reaction and facilitating the degradation; second, the elevated temperature increased the activity of K<sub>3</sub>PO<sub>4</sub>, which accelerated the transesterification of ethanol and made it easier to attack the ester bond of SAE, thus accelerating the degradation rate. However, too high a temperature may bring a series of problems. First, high temperatures can significantly increase energy consumption and make the degradation process less economical. Second, at high temperatures, the catalyst K<sub>3</sub>PO<sub>4</sub> and degradation products are more likely to dissolve in high-boiling solvents, making it difficult for the catalyst to self-separate and requiring additional separation

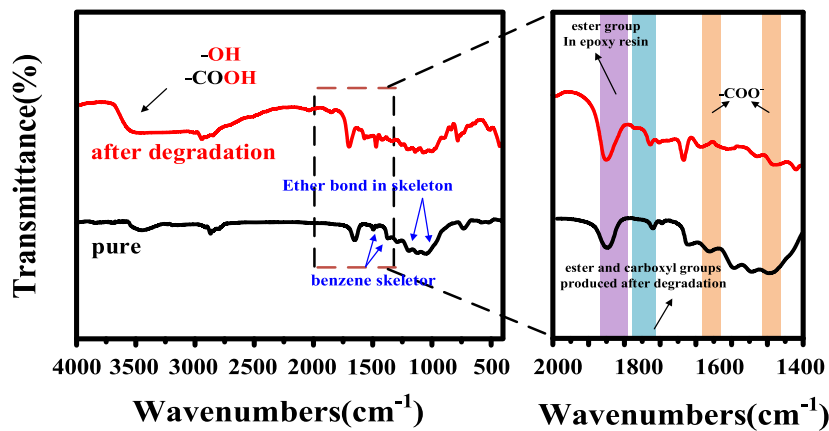


FIG. 7. FTIR spectra of pure epoxy resin and SAE's alcoholysis product.

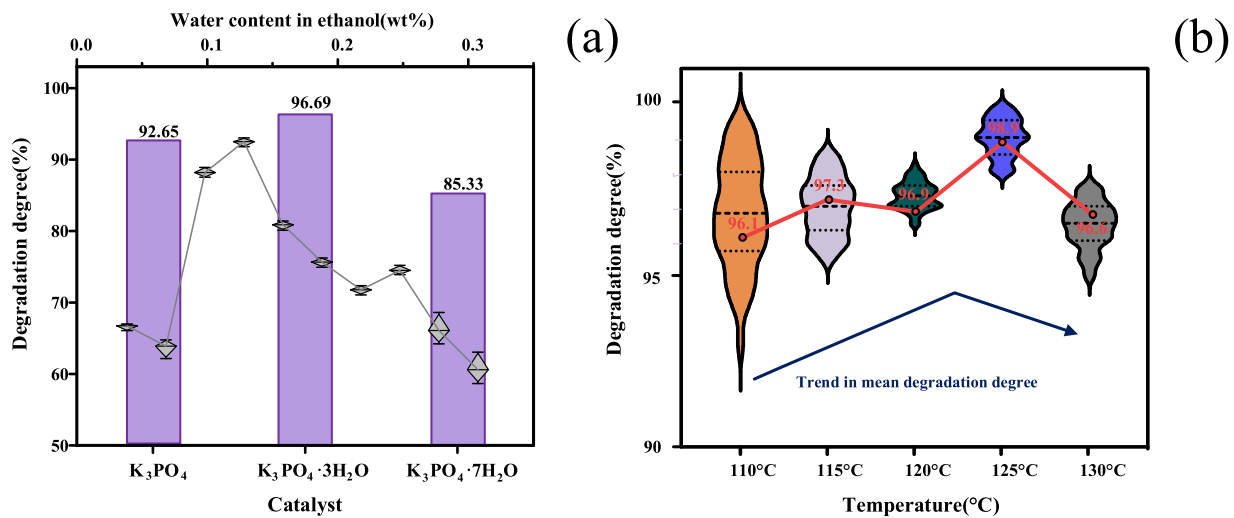


FIG. 8. (a) Effect of water content on alcoholysis. (b) Effect of temperature on alcoholysis.

steps, which increases the operational complexity and cost. In addition, too high a temperature may lead to excessive degradation and destroy the structure of the degradation product, making it difficult to reuse as a curing agent. Therefore, selecting a temperature range of 110–130 °C not only effectively degrades the epoxy resin but also reduces energy consumption, simplifies the separation process, and ensures the recoverability of the degradation products.

## VII. CONCLUSION

In this study, the electrical, mechanical, and thermal properties of  $SiO_2$ -filled anhydride-cured epoxy composites were systematically investigated and their degradation behavior under mild conditions was examined. The results show that the SAE composites maintain excellent properties even with high filler content (up to 50 wt. %), making them suitable for high-performance electrical insulation applications. The efficient alcoholysis of SAE was successfully achieved under mild conditions (120 °C, 3 h) using a

$K_3PO_4$ -catalyzed ethanol system, providing a sustainable route for the degradation and recycling of epoxy-based insulating materials. The main findings are summarized as follows:

### (1) Electrical, mechanical, and thermal properties:

The resistivity of the SAE composites decreases slightly with increasing  $SiO_2$  content, which has a minor effect on the electrical insulation properties. The dielectric constant increases with increasing  $SiO_2$  content due to enhanced polarization effect, while all the samples maintain relatively high breakdown strength suitable for insulation applications. The tensile strength is moderately enhanced with increasing  $SiO_2$  content to reach the optimum level, after which further increase (45 wt. %) leads to a slight decrease in tensile strength. Thermal analysis shows good thermal stability of the SAE composites, and the thermal decomposition temperature remains high, confirming their suitability for insulation at high temperatures.

## (2) Degradation behavior of SAE composites:

Alcoholysis of SAE composites using a  $K_3PO_4$ -catalyzed ethanol system under mild conditions ( $120^\circ C$ , 3 h) resulted in a degradation efficiency close to 100%. The experiments showed that the appropriate amount of water and temperature could significantly improve the degradation efficiency. The addition of a small amount of water increased the solubility and catalytic activity of  $K_3PO_4$ , while an appropriate increase in temperature enhanced the swelling effect of ethanol on SAE and facilitated the contact between the catalyst and reactants. However, too much water or too high a temperature could reduce the degradation efficiency. Excessive water can weaken the solvent properties, while too high a temperature may lead to the dissolution of the catalyst and degradation products and increase the difficulty of separation.

## (3) Chemical structure and degradation mechanisms:

FTIR analysis showed that the major functional groups in the SAE composites were consistent with the pristine anhydride-cured epoxy resin, and no new chemical bonds were formed between the epoxy resin and the  $SiO_2$  filler. This confirms that the  $SiO_2$  filler mainly acts as a physical reinforcement in the composites without participating in the chemical reaction. During the alcoholysis process,  $K_3PO_4$  catalyzed the ethanol to break the crosslinked ester bonds of the epoxy resin through the transesterification reaction to produce recyclable oligomers. The reduction of the intensity of the carbonyl peaks in the FTIR spectra confirms the disruption of the crosslinked structure and verifies that the SAE composites are capable of being degraded gently and efficiently at  $110$ – $130^\circ C$ . The composites are also degraded by the carbonyl peaks in the FTIR spectra.

## (4) Recovery and reuse of degradation products:

After degradation,  $K_3PO_4$ ,  $SiO_2$  filler, and epoxy resin oligomers can be separated by simple filtration and evaporation.  $SiO_2$  filler maintains its original structure and properties and can be reused directly. FTIR analysis shows that the oligomers in the degradation products have reuse potential and can be reused as raw materials in the preparation of epoxy resin.

## ACKNOWLEDGMENTS

This work was financially supported by the Natural Science Foundation of Hubei Province (Grant No. 2023AFB384).

## AUTHOR DECLARATIONS

## Conflict of Interest

The authors have no conflicts to disclose.

## Author Contributions

**Xu Zhang:** Writing – original draft (equal); Writing – review & editing (equal). **Chengjie Li:** Data curation (equal); Investigation (equal); Writing – original draft (equal); Writing – review & editing (equal). **Xianming Ye:** Data curation (equal); Investigation (equal).

**Xiaoxing Zhang:** Formal analysis (equal); Validation (equal). **Eric Maluta:** Formal analysis (equal); Validation (equal). **Yunjian Wu:** Funding acquisition (equal); Supervision (equal); Validation (equal); Visualization (equal).

## DATA AVAILABILITY

The data that support the findings of this study are available from the corresponding author upon reasonable request.

## REFERENCES

- G. Oliveux, L. O. Dandy, and G. A. Leeke, "Current status of recycling of fibre reinforced polymers: Review of technologies, reuse and resulting properties," *Prog. Mater. Sci.* **72**, 61–99 (2015).
- Y. Sun, Y. Guo, and H. Yang, "A molecular dynamics study of crosslinked epoxy networks: Construction of atomistic models," *Mol. Simul.* **46**(2), 121–127 (2020).
- C. Jehanno, J. Demarteau, D. Mantione *et al.*, "Selective chemical upcycling of mixed plastics guided by a thermally stable organocatalyst," *Angew. Chem., Int. Ed.* **60**(12), 6710–6717 (2021).
- Y. Jia, H. Li, and Z. Wang, "Research progress in treatment technology of municipal solid waste in China," *Adv. Environ. Prot.* **9**(05), 717–725 (2019).
- Y. Jing, Y. Wang, S. Furukawa *et al.*, "Towards the circular economy: Converting aromatic plastic waste back to arenes over a Ru/Nb<sub>2</sub>O<sub>5</sub> catalyst," *Angew. Chem., Int. Ed.* **60**(10), 5527–5535 (2021).
- X. Zhang, C. Ma, P. Liu *et al.*, "Recycling of ammonia-cured epoxy resin by oxidative degradation of nitric acid assisted by swelling agent," *Eur. Polym. J.* **186**, 111823 (2023).
- M. Shen and M. L. Robertson, "Degradation behavior of biobased epoxy resins in mild acidic media," *ACS Sustainable Chem. Eng.* **9**(1), 438–447 (2020).
- L. Zhang, J. Liu, W. Nie *et al.*, "Degradation of anhydride-cured epoxy resin using simultaneously recyclable solvent and organic base catalyst," *J. Mater. Cycles Waste Manage.* **20**, 568–577 (2018).
- A. Kamimura, K. Yamada, T. Kuratani *et al.*, "DMP as an effective catalyst to accelerate the solubilization of waste fiber-reinforced plastics," *ChemSusChem* **1**(10), 845–850 (2008).
- X. Zhao, X. L. Wang, F. Tian *et al.*, "A fast and mild closed-loop recycling of anhydride-cured epoxy through microwave-assisted catalytic degradation by trifunctional amine and subsequent reuse without separation," *Green Chem.* **21**(9), 2487–2493 (2019).
- X. Zhao, X. Liu, K. Feng *et al.*, "Multicycling of epoxy thermoset through a two-step strategy of alcoholysis and hydrolysis using a self-separating catalysis system," *ChemSusChem* **15**(3), e202101607 (2022).
- X. Zhao, W. Li, X. Yang *et al.*, "Effect of accelerator on properties of epoxy resin re-prepared from alcoholysis recycling," *High Voltage* **10**, 208 (2024).
- W. Zhao, L. An, and S. Wang, "Recyclable high-performance epoxy-anhydride resins with DMP-30 as the catalyst of transesterification reactions," *Polymers* **13**(2), 296 (2021).
- Standard B, ISO B, "Plastics—Determination of tensile properties—Part 1," pp. 521–527, 1996.
- A. Al Soud, S. I. Daradkeh, A. Knápek *et al.*, "Electrical characteristics of different concentration of silica nanoparticles embedded in epoxy resin," *Phys. Scr.* **98**(12), 125520 (2023).
- Y. Zhang, C. Y. Won, and C. C. Chu, "Synthesis and characterization of biodegradable network hydrogels having both hydrophobic and hydrophilic components with controlled swelling behavior," *J. Polym. Sci., Part A: Polym. Chem.* **37**(24), 4554–4569 (1999).
- A. Radoń, P. Włodarczyk, A. Drygała *et al.*, "Electrical properties of epoxy nanocomposites containing Fe<sub>3</sub>O<sub>4</sub> nanoparticles and Fe<sub>2</sub>O<sub>3</sub> nanoparticles deposited on the surface of electrochemically exfoliated and oxidized graphite," *Appl. Surf. Sci.* **474**, 66–77 (2019).
- N. Phonthamachai, H. Chia, X. Li *et al.*, "Solvent-free one-pot synthesis of high performance silica/epoxy nanocomposites," *Polymer* **51**(23), 5377–5384 (2010).

- <sup>19</sup>A. A. Soud, S. Daradkeh, A. Knápek *et al.*, “Influence of high concentration of silica nanoparticles on the dielectric spectra,” in *Proceedings II of the 29th Conference STUDENT EEICT 2023: Selected papers* (2023).
- <sup>20</sup>C. A. Ramírez-Herrera, I. Cruz-Cruz, I. H. Jiménez-Cedeño *et al.*, “Influence of the epoxy resin process parameters on the mechanical properties of produced bidirectional [±45] carbon/epoxy woven composites,” *Polymers* **13**(8), 1273 (2021).
- <sup>21</sup>X. Zhao, W. Li, Y. Zhang *et al.*, “Recycling of anhydride-cured epoxy resin through alcoholysis and its insulation property after re-preparation,” in *2023 IEEE 4th International Conference on Electrical Materials and Power Equipment (ICEMPE)* (IEEE, 2023), pp. 1–4.
- <sup>22</sup>X. Kuang, Q. Shi, Y. Zhou *et al.*, “Dissolution of epoxy thermosets via mild alcoholysis: The mechanism and kinetics study,” *RSC Adv.* **8**(3), 1493–1502 (2018).
- <sup>23</sup>A. A. A. Youssef, “The permittivity and AC conductivity of the layered perovskite [(CH<sub>3</sub>)(C<sub>6</sub>H<sub>5</sub>)<sub>3</sub>P]<sub>2</sub>HgI<sub>4</sub>,” *Z. Naturforsch. A* **57**(5), 263–269 (2002).
- <sup>24</sup>K. Funke, “Jump relaxation model and coupling model—A comparison,” *J. Non-Cryst. Solids* **172**, 1215–1221 (1994).
- <sup>25</sup>X. Zhao, W. Li, Y. Zhang *et al.*, “Performance evaluation of insulating material prepared from recycled anhydride-cured epoxy resin by alcoholysis,” *IEEE Trans. Dielectr. Electr. Insul.* **30**(6), 2724–2733 (2023).
- <sup>26</sup>C. Ang and Z. Yu, “DC electric-field dependence of the dielectric constant in polar dielectrics: Multipolarization mechanism model,” *Phys. Rev. B* **69**(17), 174109 (2004).
- <sup>27</sup>L. Zhu, “Exploring strategies for high dielectric constant and low loss polymer dielectrics,” *J. Phys. Chem. Lett.* **5**(21), 3677–3687 (2014).
- <sup>28</sup>Resin based reactive compounds used for electrical insulation—Part 3: Specifications for individual materials-sheet 1: Unfilled epoxy resinous compounds, Standard IEC 60455-3-1, 2003.
- <sup>29</sup>Z. Yutao, C. Cheng, J. Weifang *et al.*, “Relationship between dielectric loss and interphase structure of filled-type polymer composites,” in *Proceedings of 1995 International Symposium on Electrical Insulating Materials* (IEEE, 1995), pp. 77–80.
- <sup>30</sup>Basin Insulator for High-Voltage Alternating Current Gas-Insulated Metal-Enclosed Switchgear, Standard NB/T 42105, 2016.
- <sup>31</sup>S. Li, G. Yin, G. Chen *et al.*, “Short-term breakdown and long-term failure in nanodielectrics: A review,” *IEEE Trans. Dielectr. Electr. Insul.* **17**(5), 1523–1535 (2010).
- <sup>32</sup>B. Zhang, W. Gao, P. Chu *et al.*, “Trap-modulated carrier transport tailors the dielectric properties of alumina/epoxy nanocomposites,” *J. Mater. Sci.: Mater. Electron.* **29**, 1964–1974 (2018).
- <sup>33</sup>Electrical insulation-thermal evaluation and designation, Standard IEC No. 60085, 2007.
- <sup>34</sup>Y. Zheng, R. Ning, and Y. Zheng, “Study of SiO<sub>2</sub> nanoparticles on the improved performance of epoxy and fiber composites,” *J. Reinf. Plast. Compos.* **24**(3), 223–233 (2005).
- <sup>35</sup>S. Patel, R. Sengupta, U. Puntambekar *et al.*, “Effect of different types of silica particles on dielectric and mechanical properties of epoxy nanocomposites,” *Mater. Today: Proc.* **44**, 1848–1852 (2021).
- <sup>36</sup>T. H. Hsieh, A. J. Kinloch, K. Masania *et al.*, “The mechanisms and mechanics of the toughening of epoxy polymers modified with silica nanoparticles,” *Polymer* **51**(26), 6284–6294 (2010).
- <sup>37</sup>S. R. Karnati, P. Agbo, and L. Zhang, “Applications of silica nanoparticles in glass/carbon fiber-reinforced epoxy nanocomposite,” *Compos. Commun.* **17**, 32–41 (2020).
- <sup>38</sup>X. Zhang, Y. Hu, G. Wang *et al.*, “Alcohol degradation of anhydride-cured epoxy resin insulations and the properties of recycled materials,” *Polym. Degrad. Stab.* **232**, 111134 (2025).